



Experimental study on seismic performance of prefabricated replaceable beam-column connectors using double-sided angle steel

SUN. Dongde⁽¹⁾, YANG. Yong⁽²⁾

⁽¹⁾ PhD student, School of Civil Engineering, Xi'an University of Architecture and Technology, sdd1513@outlook.com

⁽²⁾ Professor, School of Civil Engineering, Xi'an University of Architecture and Technology, yyhhp2004@163.com

Abstract

An innovative performance-recoverable beam-column connection was proposed in this paper. Based on quasi-static test of two specimens without replaceable angle steel, five specimens with double-side angle steels and one specimen with one-side replaceable angle steel, the seismic performance of this new type of beam-column connector was analyzed. Through the analyses of destruction form, hysteretic loops, skeleton curves, cumulative dissipated energy, strength and stiffness degradation, residual deformation and re-centering behavior, measured strains as well as prestress development results of beam-column connector, the effects of setting angle steel, initial prestressing, different flange thickness of the connector and replacement of angle steel on the seismic performance of the prefabricated beam-column connector were examined. The results indicated that: (1) the seismic performance of this new type connector shown an excellent seismic behavior. (2) Increasing the flange thickness of the connector could effectively improve the peak load and energy dissipation capacity, but it has little effect on the initial stiffness, strength degradation and stiffness degradation. Moreover increasing the flange thickness could reduce residual deformation and improved self-reset capability. (3) The using of replaceable angle steel could effectively improve the initial stiffness, peak load and energy consumption capacity of the connector. At the same time, the replaceable angle steel also could limit the expansion of the flange of the connector. (4) Increasing the initial prestress of the specimen could significantly improve the peak load, initial stiffness and energy consumption capacity, and the self-reset capability was particularly improved. Whereas higher initial prestress had little effect on the strength degradation and stiffness degradation of the specimen. (5) For the connector with angle steel arranged on one side, it also had good test results, which could be used as a method to solve the problem of floor slab layout for deeper research. (6) Before the 3.33% angle-displacement, the re-centering rate with 100kN initial prestress specimens could reach above 0.8. Although the connector was slightly damaged during once loading, the replaceable angle steel could be easily and quickly replaced to achieve the recovery of seismic performance. The mechanism of "Self-centering under moderate earthquake and replaceable with strong earthquake" can be realized well by rational design, which will provide a good reference for practical engineering.

Keywords: self-centering, replaceable structure, beam-column connection, quasi-static test, seismic performance



1. Introduction

In recent years, the research and application about the idea of replaceable structure in building structure has gradually increased^[1-3]. Replaceable structure is to weaken or set a part as a ductile energy dissipation member in the whole structure by controlling the yield mechanism and failure mode. This makes the plastic deformation and energy dissipation occurred under the earthquake are concentrated in specific part, which protects the important components of the structure from or only slightly damaged. After the earthquake, only the energy dissipation components need to be replaced to restore the structure function. The design and setting of replaceable components is the key to the replaceable system, which is equivalent to the “fuse” in the structure. It also required to have the characteristics of strong energy consumption capacity and convenient for removal and replacement.

Scholars all over the world have carried out many researches on replaceable self-centering beam-column joints^[4-5]. Cai and Meng et al. proposed a self-centering post-tensioned precast concrete frame joint based on angle steel energy dissipation^[6]. Garlock et al. proposed a self-centering steel frame in which the upper and lower flange of the beam is connected with the column by angle steel, and the beam and column are also connected by prestressed steel strand^[7]. Guo et al. proposed a new type of self-centering prestressed concrete frame with web friction devices^[8].

All the above researches show that the beam-column joint of replaceable self-centering frame structure has numerous advantages. However, the prestressed steel strand of the above self-centering joints need to run through the column, and the anchorage is anchored at the other side of the column, which the construction difficulty will increase in case of multi-span continuous beam, and the stretching effect of the prestressed steel strand is usually unsatisfactory. Moreover, for the self-centering steel frame structure, the flange and web on the end of the beam will buckle at the same time, and the whole beam section needs to be replaced when repairing after earthquake, which will cause huge economic losses. Combined with the concept of “fuse” in replaceable system, this paper proposes a prefabricated beam-column connector with replaceable angle steel, which steel connector is set between the beam and column, shear plate at beam end is connected with the web of connector, and friction energy dissipation brass plate is set in the middle. Moreover, the steel beam and connector are connected through replaceable angle steel, and prestressed steel strands are tensioned inside to enhance the connection performance, and has the advantages of high reliability and self-centering ability. The friction energy consumption is added in this new kind of connection, and the prestressed steel strand is tensioned in the beam section to approve the convenient for construction. Because the connector is relatively independent, it can widely used in steel structure, concrete structure and composite structure. This kind of prefabricated connector with replaceable angle steel has excellent seismic performance, self-centering ability and replaceable ability. The mechanism of “self-centering under moderate earthquake and replaceable with strong earthquake” can be realized well by rational design, which can provide a good reference for practical engineering.

Based on quasi-static test of eight specimens, the seismic performance of this new type of prefabricated beam-column connector was analyzed. Through the analyses of destruction form, hysteretic loops, skeleton curves, cumulative dissipated energy, strength and stiffness degradation, residual deformation and re-centering behavior, the measured strains results as well as prestress development results of beam-column connector and prestress-displacement curves, the effects of setting angle steel, initial prestressing, different flange thickness of the connector and replacement of angle steel on the seismic performance of the prefabricated beam-column connectors were examined.

2. Experimental program

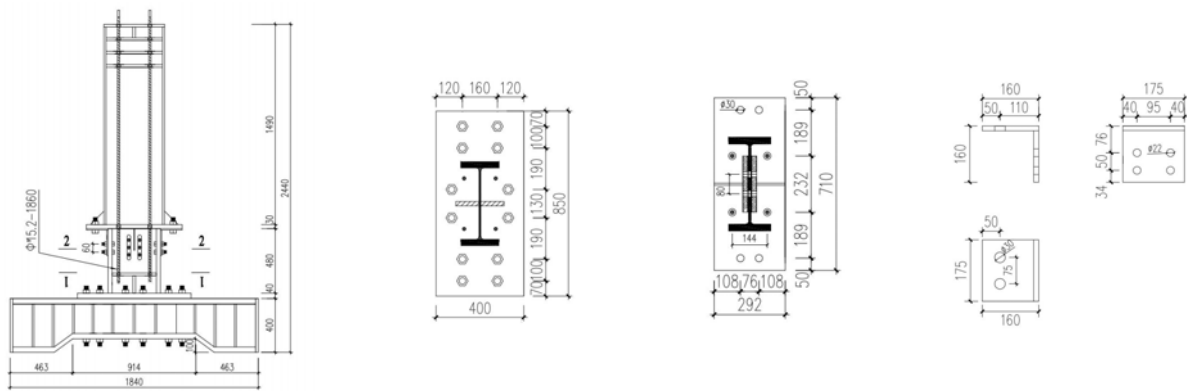
2.1 Design of testing specimens

In this paper, eight specimens were tested under low cyclic loading, including two contrast specimens without replaceable angle steel, five specimens with double-side replaceable angle steels and one specimen with one-side replaceable angle steel. The whole specimen was composed of three parts: ground beam, connector and steel beam. Friction brass plate was set at the web of beam-column connector. Different



components were connected with M12.9 high strength bolts, and the connection of steel beam and connector were enhanced by prestressed steel strand.

The total height of the specimen was 2450 mm. The sectional dimensions of beam-column connectors were divided into two types: 390mm×175mm×10mm×30mm and 390mm×175mm×10mm×20mm, with a height of 480mm. The sectional dimensions of steel beam was 400mm×200mm×10mm×20mm and with a length of 2000mm. The length, width and height of the ground beam were 1800mm, 400mm and 400mm respectively. The hot-rolled angle steel was adopted as replacement angle steel, with the dimension of 160mm×160mm×10mm and 160mm×160mm×14mm, which were made according to the design parameter. The prestressed steel strand and anchorage type were arranged with 1*7-15.24-1860 type and OVM YJM15-1 type respectively, moreover the brass plate was 3mm thick H62 type. The main parameters of each specimen are shown in Table 1, the section shape, size and structure of specimen are shown in Fig.1, and the mechanical properties of materials are shown in Table 2.



(a) Front elevation of specimen (b) 1-1 section (c) 2-2 section (d) Details of angel steel

Fig. 1 – Design and sectional dimensions of specimens

Table 1 – Parameters of specimens

Specimen No.	Replacement of specimen	Flange thickness of connector/mm	Thickness and form of angle steel/mm	Prestress/kN	Bolt pretension /N·m
SJ1	-	20	-	100	350
SJ2	-	30	-	100	350
SJ3-1	Before	30	10 (Double-side)	60	350
SJ3-2	After	30	10 (Double-side)	60	350
SJ4-1	Before	30	10 (Double-side)	100	350
SJ4-2	After	30	14 (Double-side)	100	350
SJ5	-	20	10 (Double-side)	100	350
SJ6	-	20	10 (One-side)	100	350

Note: The prestress was the initial value of each prestressed steel strand. The bolt pretension was the initial value of single bolt which applied by torque wrench.

Table 2 – Mechanical properties of materials

Sampling part	Material type	Yielding strength/MPa	Tensile strength/MPa
Steel beam	Q345	349.12	458.75
Connector web	Q235	246.55	376.83
Connector flange	Q235	252.76	394.29
Angel steel	Q235	249.45	381.53
Prestressed steel strand	1*7-15.24-1860	1659.51	1952.36



Note: Because of there was no obvious yield step in tensile curve, 85% of the tensile strength was taken as yield strength of prestressed steel strand^[11].

2.2 Test procedure and instrumentations

Fig.2 gives a view of loading device for the specimens. The lateral load was applied at the upper part of the steel beam along the horizontal direction by the MTS hydraulic servo loading system, the connector was rigidly connected with the ground beam. Lateral supports were set on two sides of loading point to prevent plane instability of steel beam. For the horizontal reversed load, the displacement control loading protocol was employed by the MTS hydraulic servo loading system in the tests. The displacement increased with one cycle at each displacement level before the displacement of 12.5mm(0.67% angle-displacement), and after it, the displacement at each level was cycled three times. The loading process was terminated when the lateral load decreased to 85% of the maximum peak load value or when the prestressed steel strand reached yield load (about 230kN). The loading system is shown in Fig.3.

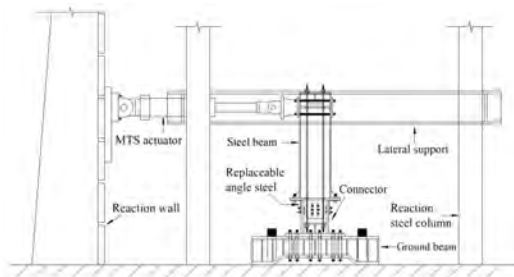


Fig. 2 – Test setup

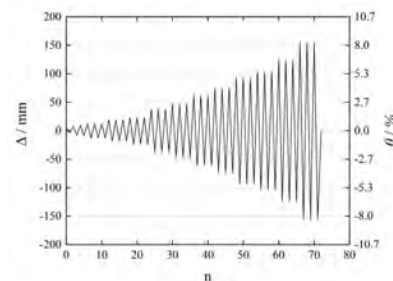


Fig. 3 – Loading protocol

A series of electrical-resistance strain gauges were arranged on the outer side of the bottom and the inside of the upper of connector flange. Four strain gauges were mounted on both connector web and replaceable angle steel. Fig.4 and Fig.5 give the layouts of the aforementioned strain gauges in detail. As shown in Fig.6, a displacement transducer (LVDT1) was placed at the lateral loading point to measure horizontal displacement of the specimen, whilst a displacement transducers (LVDT4) was arranged to measure slippage of the steel beam foundation during the loading process. The vertical displacement of the steel beam end plate was measured by two displacement transducers (LVDT2, LVDT3) to calculate the relative angle.

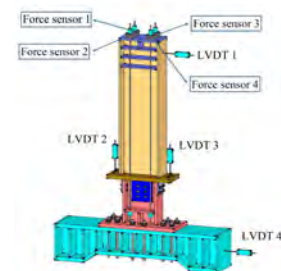
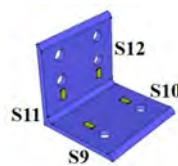


Fig. 4 – Strain gauges on connector Fig. 5 – Strain gauges on angle steel Fig. 6 – LVDT and force sensor

3. Test results

3.1 Phenomenon description

3.1.1 Specimens SJ1 and SJ2

The test phenomenon of specimen SJ1 and SJ2, which without replaceable angle steel, showed a similar failure process. Before the loading displacement of 12.5mm, two specimens were all in the elastic stage and no obvious phenomenon. When the lateral load reached the displacement of 12.5mm, the vertical gap



approximately 2mm was formed between the steel beam end plate and connector flange. After that, the push and pull sides of the connector webs of SJ1 and SJ2 showed yield at the displacement of 18.7mm and 23.4mm respectively, which indicating that the flange began to outward expand. With the increasing of loading, the sound between the shear plate and the brass plate were heard, illustrating friction was in progress to dissipate energy. With the increase of load, existing vertical gap, which between steel beam end plate and connector flange, developed rapidly to 7mm at the displacement of 37.4mm. At this time, the strain value of inside of connector flange had exceeded yield strain, whilst laser measurement showed that both sides of the flange had extended about 3mm. In addition, the prestress value was increased rapidly during loading.

when the lateral load increased to the displacement of 62.3mm, the outward expansion extent of connector flange of specimen SJ1 reached to 7mm and 5mm on push and pull side respectively, whilst the inward contraction was observed with the value of 3mm at the middle of both sides of connector flange, the flange presented S-shaped failure mode. At this time, the upper connector flange of specimen SJ2 were expanded about 4mm, but the middle part of the flange did not showed plastic deformation. Finally, when the lateral load increased to the displacement of 133.6mm, for two specimens, the upper connector flange on the push and pull sides were extended about 16mm and 6mm. Meanwhile, the maximum prestress value of the prestressed steel strands of two specimens had exceeded 230kN, which declared the loading process was terminated. The failure patterns of two specimens are shown in Fig.7(a) and (b), the expansion of connector flange is shown in Fig.7(i).

3.1.2 Specimens SJ3-1 ~ SJ5

The development of gap and failure process for specimens with double-side replaceable angle steels (specimens SJ3-1~SJ5) were generally similar to specimens without replaceable angle steel (specimen SJ1 and SJ2). Whereas the differences include three parts were as follows: (1)After three cycles at the displacement of 133.6mm, the replaceable angle steels and prestressed steel strands of SJ3-1 and SJ4-1 were replaced to form SJ3-2 and SJ4-2 respectively. (2)when the lateral load increased to the displacement of 12.5mm and 18.7mm for specimen SJ3-1, SJ3-2 and specimen SJ4-1, SJ4-2, SJ5, the measured strain of upper limb of angle steel exceeded the yield strain, and characterized that a little iron chips fall off the angle steels on both sides of the connector, which illustrated that plastic deformation of angle steels was occurred to dissipate energy under lateral low cyclic loading. With the increasing of loading, when the lateral load increased to the displacement of 62.3mm, as shown in Fig.7(g), a large distance appeared between steel beam end plate and connector flange, and the angle steels showed the failure mode of a typical flexural failure, indicating that the angle steels had fully exerted energy dissipation capacity. (3)For specimens SJ4-2, SJ5 and specimens SJ3-2, SJ4-1, the prestress value reached yield load at the displacement of 93.5mm and 133.6mm respectively. In order to research the performance in late loading stage, the specimens were loaded continuously. when the lateral load increased to the displacement of 133.6mm, the angle steel on the pull side of specimen SJ4-2 was fractured completely due to the large opening angle, and the lateral load decreased rapidly. As the test continues, the angle steel on the push side was also fractured at the displacement of 155.8mm. The failure patterns of each specimens are shown in Fig.7(c)-(g).

3.1.3 Specimens SJ6

For the test phenomenon of specimen SJ6 with one-side replaceable angle steel, when the lateral load increased to the displacement of 12.5mm, the inside of connector upper flange which side without angle steel was yield by tension, and outward expansion was occurred slightly due to compression. The connector web of set angle steel side was also yield by tension at the displacement of 18.7mm. After that, at the displacement of 37.4mm, compared with the flange without angle steel expanded about 3mm, the flange of the side set angle steel expanded only 1mm because of the limitation of angle steel. At this time, slight inner bulge were appeared in the middle of both sides of connector flange. With the increasing of loading, the disparity in expansion on two sides flange of connector became increasingly apparent, and the final disparity was approximate 4mm at the displacement of 133.6mm, whilst the maximum prestress value had exceeded 230kN, which declared the loading process was terminated. The failure patterns and flange deformation on two sides of connector of specimens SJ6 are shown in Fig.7(h) and Fig.7(k).

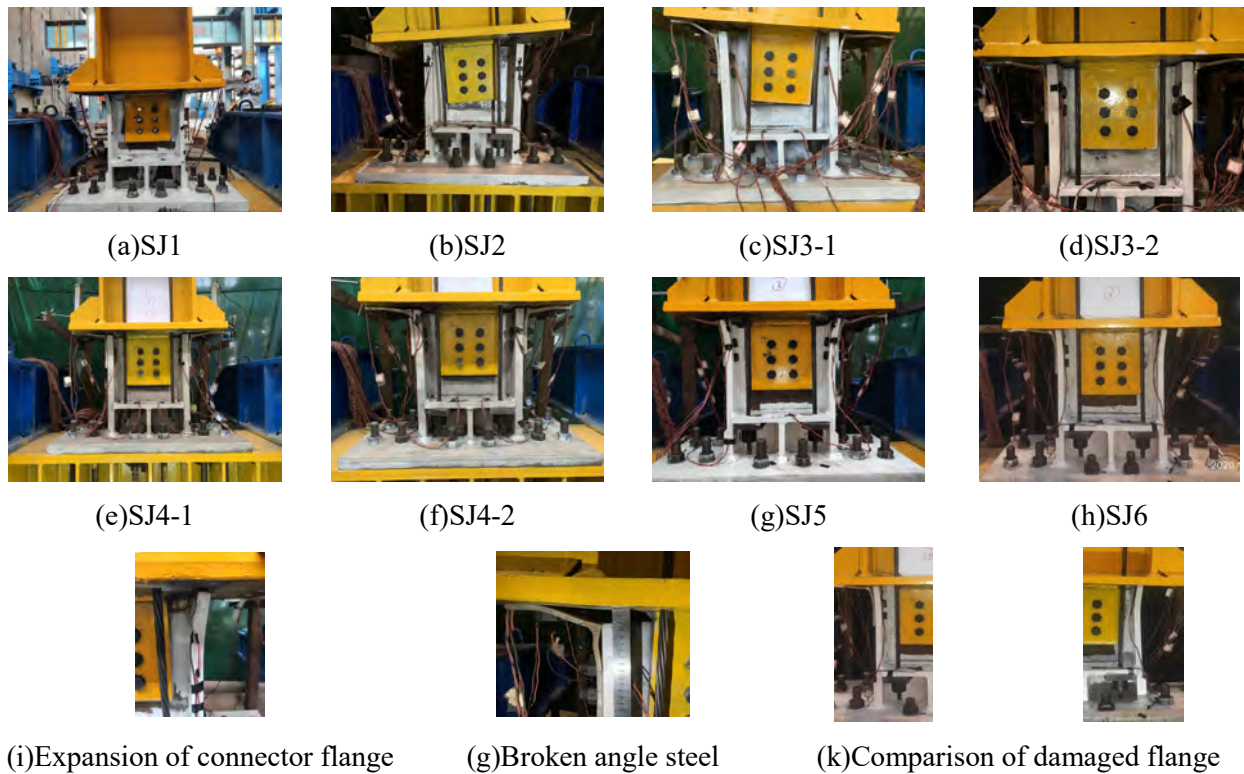


Fig. 7 – Failure modes of specimens

3.2 Hysteretic curve

Fig.8 depicts the measured horizontal load versus top displacement hysteretic curves for all the specimens. As shown in Fig.8: (1) Before the displacement of 12.5mm, the hysteresis curves of each specimen created by forward and backward loading presented the straight line shape, no significant residual deformation, little energy dissipation and satisfactory self-centering. After the loading displacement of this stage, the hysteresis curves gradually deviated from the straight line with accelerating deformation, and accompanied with the area of the hysteresis loop created by forward and backward loading increased, and the energy dissipation capacity was also increased. According to the Chinese code of GB 50011-2010^[12] that the limit value of elastic-plastic inter-story displacement angle is 1/50(2.00%) for checking elastic-plastic deformation of weak layer of multi-storey and high-rise steel structure under rare earthquake. However, before the loading displacement of 37.4mm(2.00% angle-displacement), the hysteretic curves of each specimen was provided with a typical “double flag” type, which showing a good self-centering ability. Therefore, from the hysteretic curves of specimens, the mechanism of “self-centering under moderate earthquake” could be well achieved. (2) The hysteresis curve of specimen SJ3-2 showed distinct pinch phenomenon obviously, which was not appeared in specimen SJ3-1 because of the cumulative damage of connector and brass plate were existed after once loading. Compared with specimen SJ4-1, owing to contribution of thicker angle steel, specimen SJ4-2 presented higher load-carrying capacities and plumper hysteresis loops. However, with the increase of angle steel thickness, the internal defects of material was increased simultaneously, which caused angle steel break suddenly, and bearing capacity of SJ4-2 decreased rapidly. Therefore, the mechanism of “replaceable with strong earthquake” could be achieved for this kind beam-column connector, and the seismic performance could also be improved by using thicker angle steel to achieve the repairment after earthquake. (3) From the comparison of specimens SJ3-1 and SJ4-1, SJ4-1 showed the higher peak load, greater diagonal slope and larger hysteresis loop area, which illustrated that increasing initial prestress could improve the load-carrying capacity, stiffness and energy consumption. Moreover, according to the hysteretic curve in Fig.8(h), the influence of setting angle steel or not in one specimen could be obtained. Compared with the pull part of hysteretic curve, the push part which was set



angle steel showed more satisfactory plumpness and higher load-carrying capacity, especially at the stage after the displacement of 74.8mm.

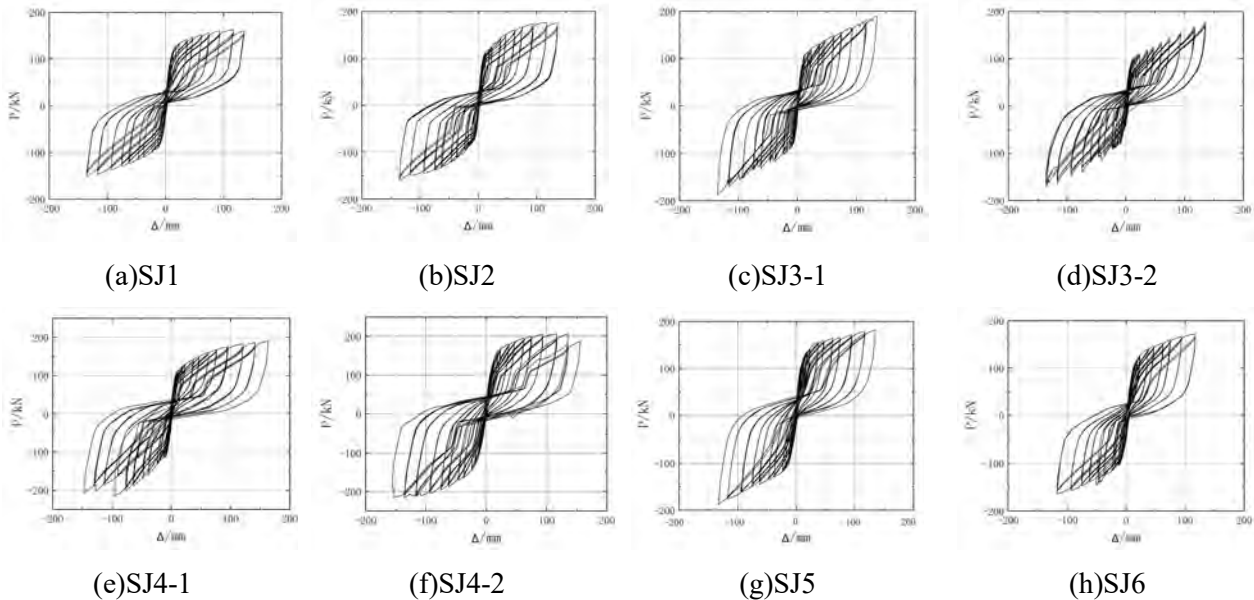


Fig. 8 – Hysteretic loops

4. Analysis of seismic performance

4.1 Skeleton curve

Fig.9 shows the skeleton curves for all specimens, and the experimental results at main stage are recorded in Table 3. As shown in Fig.9(a), when the flange thickness increased by 10mm, the peak load of specimen SJ2 and SJ4-1 increased by 6.5% and 8.6% than SJ1 and SJ5 respectively. As indicated in Fig.9(b), compared with specimen SJ3-1, after once loading, the peak load of specimen SJ3-2 decreased by 6.5%. However, as the thicker 14mm angle steel was set after once loading, horizontal load of specimen SJ4-2 increased rapidly and the later-stage of the skeleton curve moved at a gentle rate as the displacement increased, finally the peak load increased by 5.1% than SJ4-1. It indicated that thicker angle steel could compensate the performance of damaged connector, which could achieve the recovery after earthquake. In addition, it can be seen in Fig.9(c) that the peak load and initial stiffness showed the relationship of $SJ5 > SJ6 > SJ1$, which indicated that using angle steel had significant effect on bearing capacity and initial stiffness, and the effect increased with the increase of angle steel number. Moreover, from Fig.9(d), the horizontal load and stiffness of specimen SJ4-1 with 100kN initial prestress were higher than SJ3-1 with 60kN initial prestress during whole stage of test, and the peak load increased by 6.5%, which illustrating that the higher prestress could effectively improve the carrying capacity and stiffness.

4.2 Energy dissipation

Table. 4 shows the energy dissipating capacity of various specimens which were obtained by ORIGIN. It can be seen from the Table. 4 that the energy dissipation of specimens SJ2 was 11.4% higher than SJ1 counterpart because of using thicker connector flange. Whereas for specimens SJ4-1 and SJ5 with double-side angle steels, the flange expansion was limited by angle steel, therefore the influence of flange thickness on energy dissipation was unobvious^[10]. Table. 4 also shows that the energy dissipation of specimens SJ3-2 was 19.8% lower than SJ3-1, indicating that abrasion of brass plate and damage of connector would significantly decrease the energy dissipation capacity. However, the total energy consumption of SJ4-2 was 13.3% higher than that of SJ4-1, owing to the excellent energy dissipation ability of thicker angle steel. It was noted that the energy consumption disparity between SJ4-2 and SJ4-1 under each loading displacement increased gradually after the displacement of 74.8mm, which illustrated that the energy consumption of



angle steel was concentrated in later stage. Therefore, the energy consumption of angle steel and mechanism of “replaceable with strong earthquake” could be fully utilized and realized simultaneously. Moreover, the total energy consumption of SJ4-1 was 9.8% higher than that of SJ3-1, indicating higher initial prestress had favorable energy dissipation capacity.

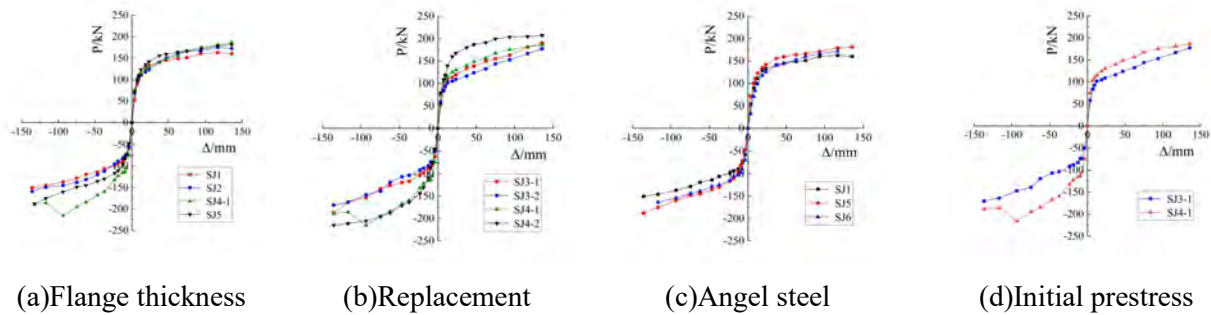


Fig. 9 – Skeleton curves

Table 3 –Experimental result at main stage

Specimen No.	P_{IGO}/kN	P_y/kN	$\Delta y/mm$	P_u/kN	$\Delta u/mm$
SJ1	55.35	-	-	156.80	135.66
SJ2	61.26	-	-	167.03	135.56
SJ3-1	56.33	88.89	13.34	188.56	135.56
SJ3-2	57.6	104.64	17.33	173.88	135.84
SJ4-1	78.91	109.51	11.57	200.84	154.08
SJ4-2	76.72	157.18	18.41	211.17	155.79
SJ5	70.27	126.08	21.03	184.85	133.98
SJ6	59.29	99.46	12.44	167.82	116.89

Note: P_{IGO} was the average load value of push and pull when the vertical gap formed between steel beam end plate and connector flange. P_y and Δy were yielding load and yielding displacement of angel steel. P_u and Δu were peak load and ultimate displacement.

Table 4 –Energy dissipation of specimens

Specimen No.	12.5mm/J	18.7mm/J	37.4mm/J	74.8mm/J	93.5mm/J	133.6mm/J	Total/J
SJ1	2472	5153	13901	29671	37659	44639	184006
SJ2	2753	5131	14107	33409	43419	52192	205003
SJ3-1	2838	5462	14856	30514	39744	51546	196732
SJ3-2	3356	5109	12132	27188	28363	35956	164152
SJ4-1	2233	4301	15920	37482	45090	52605	216003
SJ4-2	2069	4732	15719	40576	52937	66959	244823
SJ5	1971	4831	15280	34200	44968	55898	213780
SJ6	2681	5435	14780	32532	42097	51604	207207

4.3 Strength degradation and stiffness degradation

The strength degradation of specimens under cyclic loading can be evaluated by the degeneration coefficient (ϕ), which is expressed as follows:

$$\phi = \frac{P_{jmin}}{P_{jmax}} \quad (1)$$

Where P_{jmax} and P_{jmin} are the peak load value in first and third loading cycle in the case of i_{th} displacement loading level respectively. The effect of the displacement on strength degradation of various specimens are presented in Fig.10. The strength degeneration curves for various specimens decreased with



the increasing lateral displacement level. For specimens SJ1 and SJ2, the strength degradation showed slightly decrease, which were almost a horizontal line, only 4.8% and 6% at the last loading displacement. From an overall perspective, the strength degeneration coefficient of specimens with replaceable angle steels were consistently less than SJ1 and SJ2, which suggested that angle steels had adverse effect on strength degradation. Moreover, the degeneration degree of specimens with double-side angle steels was higher than SJ6, which indicated that the increase of angle steel quantity would aggravate the adverse effect. Compared with the specimens SJ3-1, SJ4-1 and SJ5, It can be seen that increasing the initial prestress and the flange thickness had little effect on strength degradation.

In this paper, stiffness is defined as the slope of the line connecting the extreme loading points in both directions of the lateral load-displacement curve for a given cycle, and can be calculated with the following equation:

$$K_i = \frac{|+F_i| + |-F_i|}{|+x_i| + |-x_i|} \quad (2)$$

Where F_i is the peak load value in the i_{th} cycle, x_i is the displacement value of the peak load point in the i_{th} cycle. The degradation curves of stiffness for various specimens are presented in Fig.11, generally, from the beginning of loading, the stiffness decreased rapidly until the gap was appeared between the contact interface of connector and steel beam end plate. After yielding of angle steel or connector, the curves moved at a gentle rate. There was no significant difference among specimens SJ1, SJ2 and SJ4-1, SJ5, and the curves almost coincided, which illustrated flange thickness had slight effect. It was noticeable that the specimens SJ5 and SJ4-1 showed relatively higher values of initial stiffness than SJ1 and SJ3-1 respectively, due to the angle steels and higher initial prestress. However, these had little effect on the trend of stiffness degradation. The specimen SJ3-2 which connector experienced once loading, showed less stiffness value than SJ3-1, especially before the loading displacement of 62.3mm. Whereas, the initial stiffness of specimen SJ4-2 was significantly higher than SJ4-1, and with a stable trend in later stage because of the 14mm thick angle steels were using after replacement.

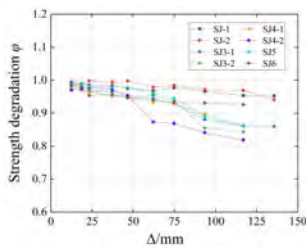


Fig. 10 – Degradation rate of bearing capacity

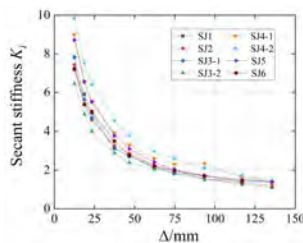


Fig. 11 – Degradation curves of stiffness

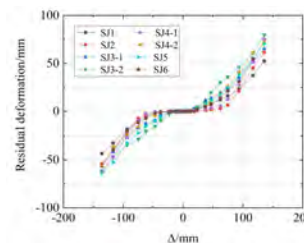


Fig. 12 – Residual deformation of specimens

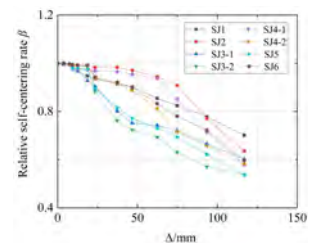


Fig. 13 – Re-centering capability of specimens

4.4 Residual deformation and self reset ability

For the replaceable structure, reducing the residual deformation is conducive to the replacement after earthquake. Fig.12 showed the relationship between residual deformation and loading displacement, the residual deformation curves for all specimens increased with the increasing lateral displacement level. In general, the residual deformation of the specimens with angle steel mainly came from the plastic deformation of angle steel, and increased with the increase of the thickness and quantity of angle steel. Whereas the residual deformation of the specimens without angle steel was mainly came from the abrasion of brass plate and the loss of prestress. In the early stage after yielding, the residual deformation of specimen SJ1 was larger than SJ2 evidently due to the fact that the thinner flange would produce more expansion deformation. Moreover, from the comparison of specimens SJ3-1 and SJ4-1, it can be seen that when the displacement was 23.4mm and 46.8mm, the residual deformation was 2.24mm and 2.12mm respectively, which showed higher initial prestress also could slow down the generation of residual deformation.



The relative self-centering rate is an important index to reflect the re-centering behavior of the specimens, which is expressed as follows:

$$\beta = 1 - \frac{\Delta_{res}^+ - \Delta_{res}^-}{\Delta_m^+ - \Delta_m^-} \quad (3)$$

The Δ_{res}^+ , Δ_m^+ and Δ_{res}^- , Δ_m^- are the residual deformation and maximum displacement of each loading cycle under push side and pull side respectively. Fig.13 showed the relationship curve between the self-centering rate and displacement of various specimens. It can be seen that the self-centering rate of specimens showed $SJ1 > SJ6 > SJ5$, which indicated that setting angle steel limited the re-centering ability. The self-centering rate of specimen SJ3-2 was characterized much lower value than SJ3-1 because of residual deformation was existed after once loading. Whilst, from the comparison of specimens SJ4-1 and SJ4-2, it can be seen that the self-centering rate decreased rapidly with replacing thicker angle steel after once loading. Moreover, it is obvious that specimen SJ4-1 exhibited favorable self-centering rate than specimen SJ3-1, which could be attributed to the higher initial prestress. However, after the displacement of 62.3mm, due to the rapid rise of prestress, the loss of prestress also increased correspondingly, which caused a sudden decline trend of self-centering rate. It is noteworthy that before the displacement of 37.4mm(2.00% angle-displacement) and 62.3mm(3.33% angle-displacement), the relative self-centering rate of SJ3-1, SJ3-2 and SJ4-1, SJ4-2 could also reach more than 0.8 respectively, which would well realize the mechanism of “self-centering under moderate earthquake”.

4.5 Strain results

Fig.14 shows the typical strain-load relationship of the specimens. The stirrup strain can directly reflect the development of plastic deformation of connector. As shown in Fig.14(a), at the beginning of loading stage, it can be seen that the strain on the inside of the upper connector flange was characterized by the alternatively positive and negative variations under cyclic loading. With the increase of loading displacement, the strain of both sides of flange were in tension state, and developed into tensile yielding gradually. It was also noticeable that the strain value increases rapidly after entered the plastic stage, which was consistent with the phenomenon of observed outward expansion. Fig.14(b) and (c) presented the strains obtained by the strain gauges of connector upper web of west and east side respectively. Generally, under the action of push and pull loading, the strain-load curves of the two sides showed a symmetrical shape. The results showed that the web seriously yielded both in tension on two sides at the test end stage, which also denoted that the final failure was not dominant by compression.

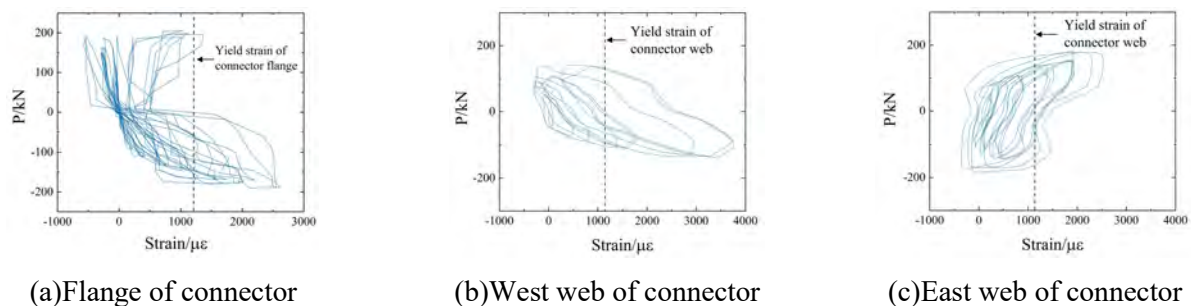


Fig. 14 –Strain of connector flange

4.6 Prestress analysis

The processes of the prestress development of each specimen is roughly the same during the test. In this paper, as illustrated in Fig.15, prestress-displacement curves of SJ1, SJ3-2 and SJ6 were given by the average prestress of two prestressed steel strands on each side of push and pull. It can be seen that the prestress value on two sides along the loading direction increased alternately and roughly symmetrical except the specimen SJ6 with one-side replaceable angle steel. The loss of prestress occurred during the loading process, which was mainly composed of two parts: The first one was caused by the slippage of anchorage,



which became more aggravating with the increase of loading displacement. Other part was caused by plastic deformation of the connector such as the flange expansion^[9-10]. Generally, every specimen showed a large loss of prestress after loading tests, however from the comparison with Fig15(b), the loss value under each loading cycle of specimen with 60kN initial prestress were less than those with the 100kN initial prestress, indicating higher prestress will lead to greater losses. The loss of prestress played a significant role on the realization of self-centering, which could aggravate the residual deformation and reduce the self reset ability. It was noticeable that the loss value of each specimen was only 9% of initial prestress at displacement of 37.4mm(2.00% angle-displacement), indicating that the mechanism of “self-centering under moderate earthquake” could be well realized.

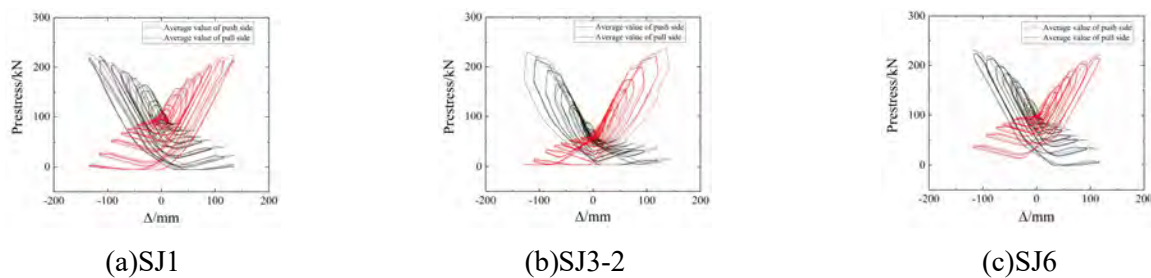


Fig. 15 –Prestress-displacement curves of specimens

4.7 Replacement analysis

Fig.16 gives the comparison of hysteretic curves from once loading and after replacement loading, the hysteretic curves of SJ3-1, SJ3-2 and SJ4-1, SJ4-2 showed slightly different. As shown in Fig.16(a), compared with specimen SJ-1, the hysteresis curve of SJ3-2 was enveloped, suffered a dramatic decrease in seismic performance such as bearing capacity, stiffness and energy consumption because the plastic cumulative damage was existed after once loading. Meanwhile, in Fig.16(b), the hysteresis curve of SJ4-2 enveloped that of SJ4-1 due to thicker 14mm angle steel set in connector could significantly enhance the seismic performance, and the specimen SJ4-2 would suffer a increased rigid and capacity both in load and deformation. It can be seen from the previous analysis that the loss of prestress was large and the connector showed different degrees of plastic deformation after once loading, but combined with the code GB50011-2010^[12], at 2.00% angle-displacement, this value of specimens SJ3-1 and SJ4-1 were smaller, which illustrated that the specimens had satisfactory self reset ability and residual deformation to replace the damaged angle steel fast and conveniently.



Fig. 16 –Comparison hysteretic loops before and after replacement

5. Conclusions

The seismic behaviors of prefabricated replaceable beam-column connectors using double-sided angle steel have been investigated in this paper. A total of eight specimens were tested under lateral cyclic load. The main conclusions drawn from this paper are as follows:

(1) Compared with the contrast specimens SJ1 and SJ-2, specimens with angle steel showed better performance on the initial stiffness, peak load and energy dissipation capacity, and the increasing range was



proportional to the angle steel quantity. Oppositely, angle steel also had a negative effect on the strength degradation and self reset ability. (2)The peak load and energy dissipation capacity of specimens could be improved by increasing the connector flange thickness, which also could effectively restrain the flange expansion to reduce the residual deformation and improve the self reset ability. However, the effect of thicker flange on the initial stiffness, strength and stiffness degradation was insignificant. (3)The specimens with 100kN initial prestress exhibited better performance than those of 60kN initial prestress both in initial stiffness, peak load, energy dissipation capacity and self reset ability, indicating that prestress played an important role in seismic behavior. Whereas, after the displacement of 62.3mm, due to the rapidly rose of prestress, the loss value increases correspondingly, and the self reset ability showed a sudden decline trend. (4)Compared with the specimens under once loading, although the seismic performance of SJ3-2 was obviously decreased, SJ4-2 had a satisfactory result due to the effective seismic performance of 14mm thick angle steel had been fully played, which was a good way to recover the performance. (5)For the specimen with one-side replaceable angle steel, it had good test results, which could be used as a method to solve the problem of floor arrangement for future study. (6)Before the displacement of 62.3mm(3.33% displacement angle), the self-centering rate of specimens with 100kN initial prestress could reach more than 0.8, which realized the mechanism of “self-centering under moderate earthquake”. Moreover for the specimen with 100kN initial prestress under once loading, the average residual deformation on push and pull sides was only 2.12mm at the displacement of 46.8mm(2.50% angle-displacement), which met the requirement of checking elastic-plastic deformation of weak layer under rare earthquake of Code for seismic design of buildings of China (GB50011-2010)^[12], and the damaged angle steel could be replaced easily and quickly to realize the mechanism of “replaceable with strong earthquake”.

6. References

- [1] Wolski M, Rides J M, Sause R (2009): Experimental Study of a Self-Centering Beam-Column Connection with Bottom Flange Friction Device. *Journal of Structural Engineering*, **135** (5), 479-488.
- [2] Sang-Hoon Oh, Young-Ju Kim, Hong-SikRyu (2009): Seismic performance of steel structures with slit dampers. *Engineering Structures*, **31** (9), 1997-2008.
- [3] Garlock M, Rides J, Sause R (2003): Cyclic load tests and analysis of Bolted top-and-seat angle connections. *ASCE Journal of Structural Engineering*, **129** (12), 1615-1625.
- [4] Rojas P, Ricles J M, Sause R (2005): Seismic Performance of Post-tensioned Steel Moment Resisting Frames With Friction Devices. *Journal of Structural Engineering*, **131** (4), 529-540.
- [5] ZHONG Xun, MENG Shaoping, PAN Qijian (2012): Experimental study on seismic performance of Post-Tensioned prestressed precast concrete beam-column assemblages. *China Civil Engineering Journal*, **45**(12), 38-44.
- [6] CAI Xiaoning, MENG Shaoping (2016): Numerical analysis for seismic behavior of self-centering post-tensioned precast beam-to-column connections. *Engineering Mechanics*, **33** (03), 143-151.
- [7] Garlock M M, Sause R, Ricles J M (2007): Behavior and Design of Posttensioned Steel Frame Systems. *Journal of Structural Engineering*, **133** (3), 389-399.
- [8] GUO Dan, SONG Lianglong (2014): Performance-based seismic design method of self-centering prestressed concrete frames with web friction devices. *Journal of Building Structures*, **35** (02), 22-28.
- [9] GARLOCK M (2002): Design, analysis, and experimental behavior of seismic resistant post-tensioned steel moment resisting frames. Bethlehem: Lehigh University.
- [10] FENG Shiqiang, YANG Yong, XUE Yicong (2020): Performance-based seismic design method of self-centering prestressed concrete frames with web friction devices. *Journal of Building Structures*, Published online, 1-11.
- [11] GUO Zhenhai (2013): Principles of reinforced concrete. Beijing: Tsinghua University Press.
- [12] Code for seismic design of buildings (2003): GB 50011-2010. Beijing: China Architecture and Building Press.